

Adaptive Safe Control for Driving in Uncertain Environments

Siddharth Gangadhar^{1†}, Zhuoyuan Wang^{1†}, Haoming Jing¹, and Yorie Nakahira^{1*}

Abstract—This paper presents an adaptive safe control method that can adapt to changing environments, tolerate large uncertainties, and exploit predictions in autonomous driving. We first derive a sufficient condition to ensure long-term safe probability when there are uncertainties in system parameters. Then, we use the safety condition to formulate a stochastic adaptive safe control method. Finally, we test the proposed technique numerically in a few driving scenarios. The use of long-term safe probability provides a sufficient outlook time horizon to capture future predictions of the environment and planned vehicle maneuvers and to avoid unsafe regions of attractions. The resulting control action systematically mediates behaviors based on uncertainties and can find safer actions even with large uncertainties. This feature allows the system to quickly respond to changes and risks, even before an accurate estimate of the changed parameters can be constructed. The safe probability can be continuously learned and refined. Using more precise probability avoids over-conservatism, which is a common drawback of the deterministic worst-case approaches. The proposed techniques can also be efficiently computed in real-time using onboard hardware and modularly integrated into existing processes such as predictive model controllers.

I. INTRODUCTION

Background. Driving in adverse conditions (e.g. icy roads with low traction) is challenging for both human drivers and autonomous vehicles. The vehicle parameters can vary by operating conditions, and the control strategy must adapt to changes quickly. These parameters may have significant uncertainties before their changes can be accurately estimated. The uncertainties due to unmodeled dynamics and noise in sensing, localization, and estimation can be substantial. Moreover, the vehicles' states can have unsafe regions of attractions, in which controllability and stability are significantly reduced. The likelihood of entering such regions depends on the future road condition (traction, curvature, etc.), planned maneuvers and actions, predictions of the environments, and their levels of uncertainty. Therefore, it is critical for an autonomous vehicle to adapt to changes, mediate behaviors based on uncertainties, exploit predictions, and do them in an integrated manner.

Related work. Various techniques have been developed for advanced driving assistance systems (ADASs) and au-

tonomous vehicles (AVs). Many of these techniques are developed in deterministic worst-case frameworks: H-infinity controllers [1], robust sliding mode controllers [2], [3], fuzzy logic controllers [4]–[6], and control barrier functions [7], [8]. These techniques can often be efficiently computed but require full system models and small bounded uncertainties (errors). In large uncertainties, these techniques may not perform well. Ensuring safety for all possible errors may be infeasible. The performance may not degrade gracefully for increasing uncertainties due to overly conservative actions.

When there are unknown parameters or changes in the internal and external parameters, techniques have been developed for parameter estimation and fast adaptation. Some combine parameter estimates (e.g., Kalman filter, Bayesian filter) and additional modifications in control to account for uncertainties [9]–[11]. The modification in control techniques is often built on worst-case frameworks and similarly assumes the availability of accurate estimates. Others directly estimate the control parameters using PID tuning [12], [13], interactive learning methods [14]–[16], adaptive control [17]. These methods' performance guarantees (convergence) often require the system dynamics to take some specific structures, and they often do not exploit future predictions.

Various model predictive control (MPC) techniques have been developed to better exploit future predictions and balance different performance objectives [18]–[22]. These methods look into future time horizons and use predictions to achieve better performance. As the number of possible trajectories grows exponentially to the outlook time horizon, there are often stringent tradeoffs between outlook time horizon and computation burdens.

To better account for uncertainties, many methods use stochastic frameworks. Examples of these techniques are stochastic MPC [23] and chance-constrained MPC [24]. Control of distributions and constraints of probability can be efficiently computed under certain assumptions such as linear dynamics and Gaussian disturbances. However, for general (nonlinear) systems, there do not exist lightweight algorithms suitable for online or onboard computation. The tradeoff between outlook time horizon and computation load can be even more stringent because constraining long-term probability requires characterizing the evolution of complex state distributions over time.

Our contributions. Motivated by these challenges, we propose a stochastic adaptive safe control technique that accounts for internal parameter changes, planned vehicle control, and the prediction of environmental factors. The technique efficiently (myopically) finds a control action with ensured long-term safe probability. The method can both

This project is funded in part by the CONIX Research Center (one of six centers in JUMP, a Semiconductor Research Corporation program sponsored by DARPA), Carnegie Mellon University's Mobility21 National University Transportation Center (which is sponsored by the US Department of Transportation), and JST PRESTO Grant Number JPMJPR2136 from Japan.

[†]These authors contributed equally.

¹Siddharth Gangadhar, Zhuoyuan Wang, Haoming Jing, and Yorie Nakahira are with the Department of Electrical and Computer Engineering, Carnegie Mellon University, {sgangadh, zhuoyuaw, haomingj, ynakahir}@andrew.cmu.edu.

*To whom correspondence should be addressed.

flexibly adapt to changes and remain robust in a steady state by mediating behaviors based on the levels of parameter uncertainties. The long-term safe probability can represent a variety of performance/safety specifications, and its probability measure can be continuously learned based on driving data.

Specifically, we derive a sufficient condition for controlling the safe probability within a desirable range. The safety condition is then used to construct a safe control algorithm that can be efficiently computed in real-time and modularly embedded into existing decision-making processes. The algorithm accounts for the distribution of uncertainties and finds appropriate control actions even in the presence of large uncertainties. Such features allow safer and faster responses to changes before sufficient samples become available or before the parameter estimates converge. Moreover, it can be modularly added into an existing decision-making process: for example, it can be incorporated into the MPCs to balance multiple objectives while ensuring chance-constrained safety conditions for nonlinear affine control systems without the assumption of Gaussian distributions. The resulting algorithms can properly control the long-term safe probabilities, which are defined based on future trajectories and intended control action, allowing that information to be used for producing more stable and safer action. Furthermore, the long-term safe probability can be learned continuously using past driving data, which allows the control policy to be individually fine-tuned based on its common driving conditions. By extending the outlook time horizon, preventive control actions can be executed before the system reaches a state where maintaining safety is no longer possible. Finally, the framework requires few assumptions in the choice of models: it can be adapted to different vehicle dynamics or tire models, ranging from white-box to gray-box to black-box models. The model also does not need to be differentiable—a common requirement when deterministic safe control algorithms that involve the computation of (Lie) derivatives to be applied.

The rest of this paper is organized as follow. We first present the vehicle dynamics, controller structures, and design objectives in Section II. Then, we present the proposed safe control framework and prove its performance guarantees in Section III. Finally, we present a few case studies of autonomous driving in Section IV and discuss the advantages of the proposed approaches.

II. PROBLEM STATEMENT

In this section, we introduce the generic vehicle dynamics in section II-A, controller in section II-B, and the safety specifications in section II-C.

A. Vehicle Dynamics

We use $x \in \mathbb{R}^m$ to represent the state of the vehicle and $u \in \mathbb{R}^n$ to represent the control action. The dynamics of x depends on the physics and mechanics of the vehicle and the control action. We use

$$\dot{x} = F_x(x, \xi) + F_u(x)u, \quad (1)$$

with some possibly nonlinear functions F_x, F_u to represent the dynamics. The vehicle dynamics are parameterized by $\xi \in \mathbb{R}^l$. The values of ξ can change over time, so its exact values may not be accessible by the controller. The system dynamics in (1) is affine to the control action u . The proposed technique is agnostic to the choice of vehicle models, and thus F_x and F_u can be high-dimensional and highly nonlinear functions and/or built from data.

In order to implement the controller in digital systems, we discretize (1) as follows.

$$x_{k+1} = F(x_k, u_k, \xi_k). \quad (2)$$

Let (2) be the discretized system dynamics, where F is a function derived from (1). Let x_k and u_k be the value of x_t and u_t evaluated at the discrete time point $t = k\Delta t$, respectively, where Δt is the sampling time of the digital controller.

B. Nominal controller

We assume the existence of an estimator for the vehicle parameters ξ . Let $\hat{\xi}_k$ denote the latest estimate of ξ available at time step k . We allow the estimator to operate in different time scale from the controller or be updated intermittently. We additionally assume that the estimator gives the posterior of the estimate. Let z denote the vehicle state and estimated parameter at time k , *i.e.*,

$$z_k = [x_k^T, \hat{\xi}_k^T]^T \in \mathbb{R}^{m+l}. \quad (3)$$

The distribution of z_k is determined from the vehicle dynamics, the estimator, and environmental changes.

The system is equipped with a nominal optimization-based (MPC) controller of the following form:

$$u_{k:k+H} = \arg \min_{u_{k:k+H} \in \mathcal{U}} J(x_{k:k+H}, u_{k:k+H}) \quad (4a)$$

$$\text{s.t. } C(x_{k:k+H}, u_{k:k+H}) \succeq 0 \quad (4b)$$

$$x_{i+1} = \hat{F}(x_i, u_i, \hat{\xi}_k), i = k, \dots, k+H \quad (4c)$$

where $x_{k:k+H} = \{x_k, x_{k+1}, \dots, x_{k+H}\}$, and $u_{k:k+H} = \{u_k, u_{k+1}, \dots, u_{k+H}\}$. Here, H is the MPC outlook horizon, and the optimization domain \mathcal{U} is the admissible set of control actions. In this optimization problem, the cost function $J(x_{k:k+H}, u_{k:k+H})$ for system state and control is minimized. Condition (4b) represents the constraints in the vehicle states and controls (*e.g.*, steering angle limits). The left hand side of (4b), $C(x_{k:k+H}, u_{k:k+H})$, is a vector valued function of $x_{k:k+H}, u_{k:k+H}$, and the inequality of (4b) is taken point-wise. Condition (4c) accounts for the knowledge of the system dynamics, which approximates the original dynamics (2), *i.e.*, $F \approx \hat{F}$. This controller is designed based on the performance specifications of the system and does not necessarily account for the safety specifications, which is described in the next subsection.

C. Safety specifications

We represent the safe event using a set $\mathcal{S} \in \mathbb{R}^m$ defined as the 0-superlevel set of a function $\phi : \mathbb{R}^m \times \mathbb{R}^l \rightarrow \mathbb{R}$, i.e.,

$$\mathcal{S}(\xi) = \{x : \phi(x, \xi) \geq 0\}, \quad (5)$$

where the function $\phi(x, \xi)$ involves the internal state of the vehicle x and external/environmental variables ξ (e.g., friction coefficients). The safety specifications is then given by the following condition: the vehicle state stays within the safe set, i.e.,

$$x \in \mathcal{S}(\xi). \quad (6)$$

A major challenge to ensure (6) arises from the uncertainties in the system. For example, safety depends on ξ , and when it changes, the controller must adapt its action before an accurate estimate of ξ can be constructed from samples. When the uncertainty of ξ is large, it can be impossible to have (6) with probability 1. Moreover, ensuring (6) for all possible worst cases may not be feasible and/or leads to unnecessarily conservative control actions, which compromise the robustness and performance of the system. Instead, we aim to control the safety probability defined below.

Specifically, we want to ensure $x \in \mathcal{S}(\xi)$ during an outlook time window $\mathcal{T}(k) = \{k, k+1, \dots, k+T\}$ with probability $1 - \epsilon$: i.e., at any time $k \in \mathbb{Z}_+$,

$$\mathbb{P}(x_\tau \in \mathcal{S}(\xi_\tau), \forall \tau \in \mathcal{T}(k)) \geq 1 - \epsilon. \quad (7)$$

Here ϵ can be interpreted as the tolerance level for unsafe events. The outlook time horizon T should be sufficiently long to avoid myopic behaviors that are unsafe. Note that the outlook time horizon T does not need to be identical to the outlook horizon H of the MPC controller (4). The benefit of choosing different T and H will be explained later in Remark 2.

III. ALGORITHM STATEMENT

In this section, we present the proposed safety condition in section III-A, and the proposed safe adaptation algorithm in section III-B.

A. Proposed Safety and Recovery Condition

In this subsection, we propose an adaptive safe control method that exploits prediction and mediates behaviors based on the level of uncertainties. We first derive a sufficient condition that ensures safe probability based on a novel probabilistic forward invariance condition. The key novelty of this condition is that it can ensure long-term safety probability to be ensured using a myopic controller that can be computed in real-time onboard computation, while standard control barrier function (CBF) based methods often lead to unsafe behaviours because of the long tail distribution of the unsafe events. The long-term safety probability can be computed offline and be continuously learned using the driving history. The controller only needs to myopically evaluate the immediate control action using a linear constraint, which can be easily integrated into optimization-based planning and control processes (e.g., MPC [18]–[20], [23], [24]).

Let A denote the following discrete-time generator.

Definition 1 (Discrete-time Generator). The discrete-time generator A of a discrete-time stochastic process $\{y_k \in \mathbb{R}^n\}_{k \in \mathbb{Z}_+}$ with sampling interval Δt evaluated at time k is given by

$$AG(y_k) = \frac{\mathbb{E}[G(y_{k+1})|y_k] - G(y_k)}{\Delta t} \quad (8)$$

whose domain is the set of all functions $G : \mathbb{R}^n \rightarrow \mathbb{R}$ of the stochastic process.

The discrete-time generator can be considered as the discrete-time counterpart of the infinitesimal generator for a continuous-time process.

Let $\Psi(z)$ be the probability of the vehicle originating from state $z_k = z$ at time k to remain safe during outlook time horizon $\mathcal{T}(k)$, i.e.,

$$\Psi(z) := \mathbb{P}(x_\tau \in \mathcal{S}(\xi_\tau), \forall \tau \in \mathcal{T}(k) | z_k = z). \quad (9)$$

Note that, conditioned on $z_k = z$, this probability does not depend on k .¹ In order to ensure safety of the system, we propose to constrain the control action u_k to satisfy the following conditions at all time $k \in \mathbb{Z}_+$:

$$A\Psi(z_k) \geq -\gamma(\Psi(z_k) - (1 - \epsilon)). \quad (10)$$

Here, $\gamma : \mathbb{R} \rightarrow \mathbb{R}$ is a function of $\Psi(z_k) - (1 - \epsilon)$. When $\Psi(z_k) \leq 1 - \epsilon$, the value of $A\Psi(z_k)$, if positive, can be interpreted as the recovery rate. Condition (10) essentially constrains the discrete-time generator of $\Psi(z_k)$ to be lower bounded by $-\gamma(\Psi(z_k) - (1 - \epsilon))$.

Remark 1. Since function $\Psi(z_k)$ gives the safety probability of the system in the time horizon $\mathcal{T}(k)$, it encodes information of prediction on the future as well as the level of uncertainties.

We impose the following two conditions for $\gamma(q)$:

Requirement 1: $\gamma(q)$ is strictly concave or linear in q .

Requirement 2: $\gamma(q) \leq q, \forall q \in \mathbb{R}$.

Condition (10) with design requirements 1 and 2 guarantees the safe probability condition (7) to hold, as stated below.

Theorem 1. Consider the open-loop system (2). Let $\gamma(q)$ satisfy requirements 1 and 2. If the state and parameter estimation originate at $z_0 = z$ with $\Psi(z) > 1 - \epsilon$, and the control action satisfies (10) at all time, then the following condition holds:

$$\mathbb{P}(x_\tau \in \mathcal{S}(\xi_\tau), \forall \tau \in \mathcal{T}(k)) \geq 1 - \epsilon \quad (11)$$

for all time $k \in \mathbb{Z}_+$. Here, the probability is taken over z_k conditioned on $z_0 = x$, and Ψ in (9) gives the probability of safety of the future trajectories $\{z_\tau\}_{\{k+1, k+2, \dots, k+T\}}$ conditioned on z_k .

Proof. See extended version of this paper [25].

Note that the left hand side of (11) is equivalent to $\mathbb{E}[\mathbb{P}(x_\tau \in \mathcal{S}(\xi_\tau), \forall \tau \in \mathcal{T}(k))]$, where the expectation is

¹This property holds because the system dynamics in (2) is time-invariant. The functions F_x and F_u do not depend on time.

taken over z_k conditioned on $z_0 = x$, and Ψ in (9) gives the probability of safety of the future trajectories $\{z_\kappa\}_{\{k+1, k+2, \dots, k+T\}}$ conditioned on z_k .

B. Proposed Safe Adaptation Algorithm

Next, we show that $A\Psi(z_k)$ can be approximated using a linear function of u_k when the sampling interval Δt is sufficiently small. With z defined in (3), let $D(z)$ denote the first m entries of the gradient of $\Psi(z)$ evaluated at z , *i.e.*,

$$D(z) = [D^{(1)}(z), D^{(2)}(z), \dots, D^{(m)}(z)]^T \in \mathbb{R}^m, \quad (12)$$

where

$$D^{(i)}(z) = \frac{\Psi(z + \Delta^{(i)}) - \Psi(z - \Delta^{(i)})}{2\Delta}. \quad (13)$$

Here, Δ is the step size to calculate the finite difference of the safety probability, $\Delta^{(i)}$ denotes a vector that takes a scalar value of Δ in i -th entry and 0 otherwise. Note that $D(z)$ has the same dimension with the state x .

We make the following assumptions:

$$\lim_{\Delta t \rightarrow 0} \mathbb{E} \left[\frac{z_{k+1} - z_k}{\Delta t} \right] = \begin{bmatrix} F_x(x_k, u_k, \hat{\xi}_k) + F_u(x_k)u_k \\ 0 \end{bmatrix} \quad (14)$$

$$\lim_{\Delta t \rightarrow 0} \frac{1}{2\Delta t} \mathbb{E} [(z_{k+1} - z_k)^T M (z_{k+1} - z_k) | z_k] = c_k \quad (15)$$

$$\lim_{\Delta t \rightarrow 0} \frac{1}{\Delta t} \mathbb{E} [R_2(z_k, z_{k+1}) | z_k] = 0. \quad (16)$$

Here, M is a matrix of appropriate dimension, c_k is a constant c_k , and R_2 denotes the terms with order greater than 2 in the Taylor expansion of Ψ , *i.e.*, $R_2(z_k, z_{k+1}) = o(\|z_{k+1} - z_k\|^2)$. Condition (14) assumes the limit of the derivative of x equals to the dynamics with the estimated parameter, and the estimated parameter is not changing in the infinitesimal time. This holds for ordinary differential equation (ODE) systems with additive Gaussian noise, which is commonly assumed in stochastic safe control community [26], [27]. It is assumed in (14) that information about the future value of $\hat{\xi}$ is not available. Condition (15) says the second order term in the Taylor expansion of Ψ equals to some constant c_k . Note that this term does not necessarily vanish (*e.g.*, Ito's calculus), but it will not depend on u . Condition (16) implies that terms higher than third order will vanish.

Lemma 1. *Assume (14)–(16) hold. Then, the following condition holds.*

$$\lim_{\Delta t \rightarrow 0} A\Psi(z_k) = D(z_k) \cdot (F_x(x_k, \hat{\xi}_k) + F_u(x_k)u_k + c_k). \quad (17)$$

Proof. See extended version of this paper [25]

From Lemma 1, we can use sufficiently small sampling interval Δt and evaluate condition (10) using

$$D(z_k) \cdot (F_x(x_k, \hat{\xi}_k) + F_u(x_k)u + c_k) \geq -\gamma(\Psi(z_k) - (1 - \epsilon)). \quad (18)$$

Since D , F_x , F_u and Ψ are all constant given x_k and $\hat{\xi}_k$, condition (18) is linear in u , thus can be used in LQ

or convex problem without losing convexity. Therefore, it can be easily integrated into existing optimization-based controllers (*e.g.*, [28]–[31]) without much extra computational [18], [32]. For example, we can impose (18) as an addition constraints in the nominal MPC controller (4), *i.e.*,

$$u_{k:k+H} = \arg \min_{u_{k:k+H} \in \mathcal{U}} J(x_{k:k+H}, u_{k:k+H}), \quad (19a)$$

$$\text{s.t. (4b), (4c) and (18)}. \quad (19b)$$

This controller exploits prediction through both MPC forward rollout and the long-term safety probability function $\Psi(z)$ in (9), with different outlook horizon H and T , respectively.

Remark 2. The computation load of the MPC controller (4) often scales exponentially with its time horizon H . Interestingly, the safety condition (10) can be used to ensure safety during horizon T without requiring the MPC controller to extend its outlook horizon to T . Thus, if the value D in (12)–(13) is computed offline, the computation load of the MPC controller only needs to scale with $H(\ll T)$.

The overall safe control strategy is given by Algorithm 1. At each time step k , Algorithm 1 functions as follows. In line 5, it obtains from the estimator the latest estimate $\hat{\xi}_k$ for the system parameter ξ . In line 6, it evaluates the functions Ψ and D at z_k either using online or offline computation. These values can be obtained by sampling the system dynamics (1) or (2), or can be continuously learned from the past driving data. In line 7, it finds an control action u_k either using the optimization problem (19). This control action u_k is executed in line 8, and its impact on x_{k+1} is observed in line 4 at the next time step.

Algorithm 1 Safe control algorithm

- 1: Initialize Δz
 - 2: $k \leftarrow 0$
 - 3: **while** $k < K_{max}$ **do**
 - 4: Observe x_k
 - 5: Obtain $\hat{\xi}_k$ from the estimator
 - 6: Obtain $\Psi(z_k)$ and $D(z_k)$
 - 7: Find $u_k \leftarrow \text{solve } \{u_k \text{ in (19)}\}$
 - 8: Execute action u_k
 - 9: $k \leftarrow k + 1$
 - 10: **end while**
-

IV. EXPERIMENT

We evaluated the efficacy of the proposed adaptive safe control method with simulation on a four-wheel 3-DoF vehicle. The design goal is to track a reference path without slipping. We present the vehicle dynamics in section IV-A, the controller and the design specification in section IV-B, and the results and discussions in section IV-C.

A. Vehicle Model

We consider the vehicle model presented in [33] and Burckhardt's tire model based on the Kamm friction circle [34].

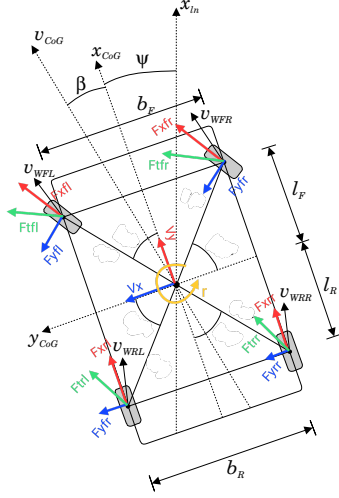


Fig. 1: Freebody diagram of the vehicle.

Fig. 1 shows the diagram of the vehicle model. In this model, each tire is associated with a longitudinal and lateral force. We use F_t to denote the total tire force on each of the four wheels, calculated as the squared sum of the lateral and longitudinal tire force. The saturated tire grip force is given by

$$F_{\text{sat}} = \mu mg/4, \quad (20)$$

where m is the vehicle mass, and g is gravitational acceleration constant, μ is the friction coefficient between the tire and road (referred to as c_1 in Burckhardt's tire model). The vehicle system's state and control actions are

$$x = [x_{CoG}, y_{CoG}, \psi, v_x, v_y, r, \omega_{fl}, \omega_{fr}, \omega_{rl}, \omega_{rr}, \delta]^T \quad (21)$$

$$u = [T_e, \dot{\delta}]^T, \quad (22)$$

where x_{CoG} , y_{CoG} , and ψ are the vehicle's inertial pose, v_x and v_y are the vehicle's frame velocities, r is the yaw rate, ω_{fl} , ω_{fr} , ω_{rl} , and ω_{rr} are the tire angular rates, δ is the steering angle, T_e is the input torque from the differential and $\dot{\delta}$ is the steering rate. The specific choice of parameters for simulation are summarized in Table I. The friction coefficient μ is the unknown parameter ξ in our simulation, by adding an additive zero-mean Gaussian noise with variance σ^2 to μ . Please see extended version of this paper [25] for more details of the vehicle model.

B. Controllers and Design Specifications

The performance specification is to track a reference trajectory. This can be achieved by a linear time-varying MPC controller (LTV-MPC) of the form (4) with

$$\hat{F}(x, u) = A_{\text{lin}} x_e + B_{\text{lin}} u_e, \quad (23a)$$

$$J(x, u) = \frac{1}{2} x_e^T Q x_e + \frac{1}{2} u_e^T R u_e, \quad (23b)$$

$$C(x, u) \leq 0, \quad (23c)$$

TABLE I: Simulation Parameters

Parameter	Definition	Value
C_f	cornering stiffness for front tire	6680 N/rad
C_r	cornering stiffness for rear tire	6680 N/rad
b_a	aerodynamic drag coefficient	100 Ns/m
b_r	tire drag coefficient	100 Ns/m
μ	tire to road friction coefficient	0.03
m	mass of the vehicle	1500 kg
g	gravitational acceleration	9.8 m/s ²
L_f	front wheel distance to vehicle center	1.070 m
L_r	rear wheel distance to vehicle center	1.605 m
W	width of the vehicle	1.517 m
I_z	rotational inertia about the center	2600 kgm ²

where $x_e = x - x_r$, $u_e = u - u_r$ with $[x_r, u_r]$ be the reference trajectory, A_{lin} and B_{lin} are the Jacobian of a reduced-order linearized vehicle dynamics at each time step, with states $x = [x_{CoG}, y_{CoG}, \psi, v_x, v_y, r]^T$ and controls $u = [\dot{v}_x, \delta]^T$ [35]. The reference trajectories $[x_r, u_r]$ are obtained from a B-spline based planner and reference generator demonstrated in [33]. The objective J is the weighted quadratic penalties on the trajectory tracking error x_e and the difference between the actual control and the reference control u_e . Constraint function C limits the control inputs of the vehicle system within a certain range. LTV-MPC linearizes the system at each time step, and predictively optimize the control input in a given horizon H to make sure the vehicle is tracking the reference trajectory while satisfying necessary constraints. However, we do not add any safety specific constraints in LTV-MPC. This is because LTV-MPC uses a reduced state space model of the vehicle and the tire force dynamic is highly nonlinear and under-actuated in this state space. Moreover, the nonlinearity of tire-force dynamics and the under-actuated nature of the safety specification prevents control barrier function methods to be used for constructing a linear constraint.

The safety specification is to limit each tire's total force within a certain percentage $\eta \in (0, 1)$ of the maximum tire force F_{sat} , beyond which the vehicle starts to slip. The safety condition is defined by (5) with

$$\phi(x, \xi) = \min \left\{ 1 - \left(\frac{4F_{tfl}}{\eta\xi mg} \right)^2, 1 - \left(\frac{4F_{tfr}}{\eta\xi mg} \right)^2, 1 - \left(\frac{4F_{trl}}{\eta\xi mg} \right)^2, 1 - \left(\frac{4F_{trr}}{\eta\xi mg} \right)^2 \right\}, \quad (24)$$

where $\xi = \mu$ is the friction coefficient, F_{tfl} and F_{trr} , etc, are the tire forces on front left wheel, rear right wheel, etc. With this definition, if any of the four tire's total force F_t exceed ηF_{sat} , function $\phi(x, \xi)$ in (24) will become negative indicating that safety is being compromised. Accordingly, the proposed controller is given by (19) whose parameters are defined by (23). This controller essentially add to LTV-MPC a linear constraint (18) that ensures the long-term safe probability and probabilistic recovery speed.

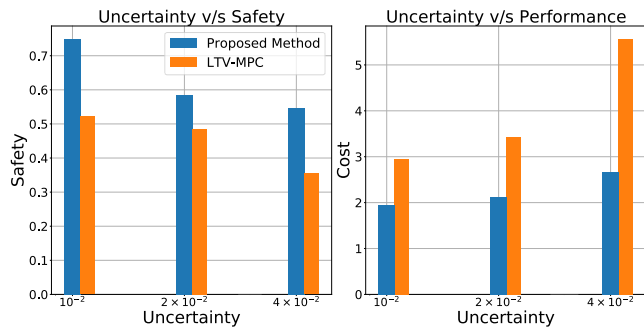


Fig. 2: Impact of uncertainty on safety (left) and performance (right).

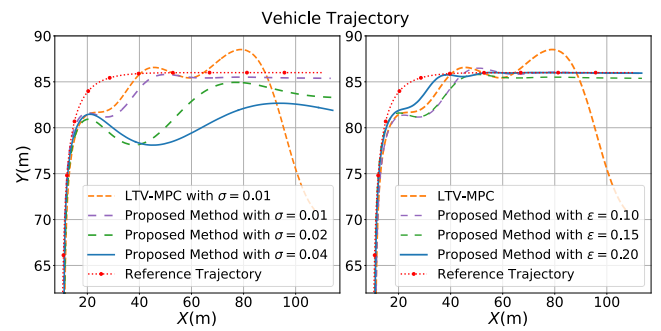


Fig. 4: Trajectory of the vehicle for varying uncertainty σ (left) and tolerance ϵ (right).

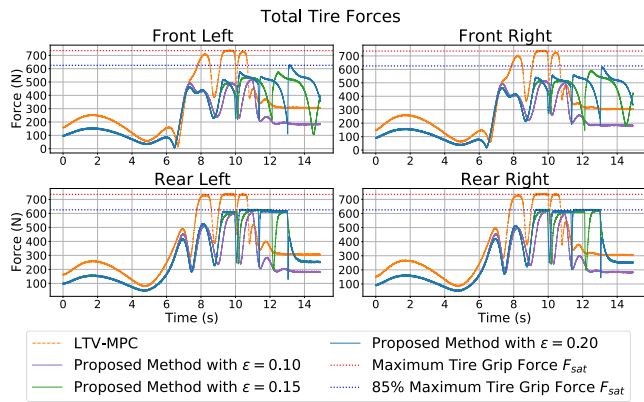


Fig. 3: Total tire force of each wheel.

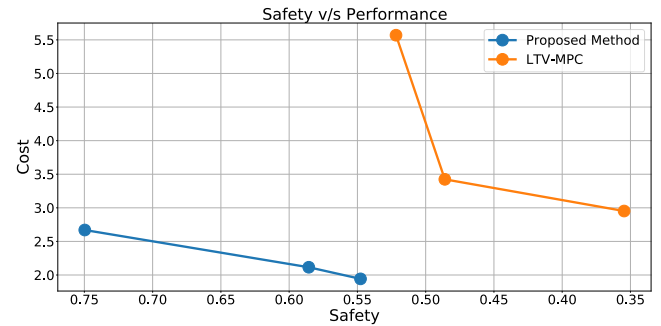


Fig. 5: Safety v.s. performance tradeoffs

C. Results

Impact of uncertainty on safety and performance. Fig 2 shows the safety and performance for varying levels of uncertainties for the proposed method and the LTV-MPC. The safety is measured by the averaged value of the safety specification function (24), the performance is measured by the averaged cost function value, and the level of uncertainty is measured by σ . In contrast to LTV-MPC, the proposed method has a more graceful degradation in safety and performance. With the proposed method, the tire force always stayed within 85% of its saturation (Fig. 3) and produced stable trajectories (Fig. 4 left). This can be achieved because the proposed controller will look into the future and impose a more effective safe control on the system once the safety probability has an tendency of dropping, i.e., the system state is getting close to some potentially unsafe regions. With LTV-MPC, the total tire force started to exceed the maximum desired saturation rate from around 8 seconds. This is because LTV-MPC can not directly account for the safety specifications in its constraints, as mentioned in the previous section.

Safety versus performance tradeoffs. Fig. 5 shows the tradeoffs between the safety and performance for the proposed method and the LTV-MPC. The proposed methods have an improved tradeoff than LTV-MPC. This is achieved because it can systematically trade-off long-term safety vs performance by varying the tolerance level ϵ . With a looser

safety requirement, more aggressive control was produced to improve performance (Fig. 4 right).

Time horizon, computation load, and safety. Fig. 6 shows the effect of the MPC outlook time horizon H and resulting computation load and safety. The computation load grows with H in the order of $O(H^3)$ [36], [37]. However, reducing H does not compromise safety because the proposed methods only requires myopic evaluation to achieve long-term safety.

V. CONCLUSION

This paper proposes a stochastic adaptive safe control technique for adverse driving conditions that can exploit prediction, mediate behaviors based on uncertainty, and adapt to changes. We demonstrate its reliability, efficiency,

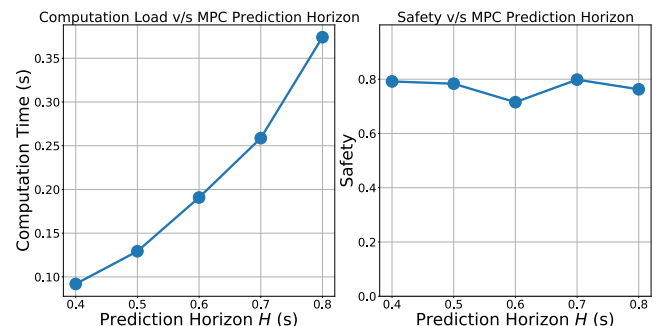


Fig. 6: Impact of MPC time horizon H on computation load (left) and safety (right).

and modularity through theoretical and numerical studies. The reliability is due to its provable guarantee of long-term safe probability or probabilistic recovery speeds. The computational efficiency of imposing chance constraints in nonlinear systems is achieved through a novel use of probabilistic forward invariance conditions. Finally, the derived safety condition can be modularly integrated into existing controllers, which largely improves its applicability.

REFERENCES

- [1] Q. Lu, A. Sorniotti, P. Gruber, J. Theunissen, and J. De Smet, "H loop shaping for the torque-vectoring control of electric vehicles: Theoretical design and experimental assessment," *Mechatronics*, vol. 35, pp. 32–43, 2016.
- [2] H.-S. TAN and Y.-K. CHIN, "Vehicle antilock braking and traction control: a theoretical study," *International journal of systems science*, vol. 23, no. 3, pp. 351–365, 1992.
- [3] L. Zhang, H. Ding, J. Shi, Y. Huang, H. Chen, K. Guo, and Q. Li, "An adaptive backstepping sliding mode controller to improve vehicle maneuverability and stability via torque vectoring control," *IEEE Transactions on Vehicular Technology*, vol. 69, no. 3, pp. 2598–2612, 2020.
- [4] M. Bauer and M. Tomizuka, "Fuzzy logic traction controllers and their effect on longitudinal vehicle platoon systems," *Vehicle system dynamics*, vol. 25, no. 4, pp. 277–303, 1996.
- [5] A. Parra, A. Zubizarreta, J. Pérez, and M. Dendaluze, "Intelligent torque vectoring approach for electric vehicles with per-wheel motors," *Complexity*, vol. 2018, 2018.
- [6] X. Wu, C. Ma, M. Xu, Q. Zhao, and Z. Cai, "Single-parameter skidding detection and control specified for electric vehicles," *Journal of the Franklin Institute*, vol. 352, no. 2, pp. 724–743, 2015.
- [7] A. D. Ames, J. W. Grizzle, and P. Tabuada, "Control barrier function based quadratic programs with application to adaptive cruise control," in *53rd IEEE Conference on Decision and Control*. IEEE, 2014, pp. 6271–6278.
- [8] S. Kolathaya and A. D. Ames, "Input-to-state safety with control barrier functions," *IEEE control systems letters*, vol. 3, no. 1, pp. 108–113, 2018.
- [9] M. Wielitzka, M. Dagen, and T. Ortmaier, "Sensitivity-based road friction estimation in vehicle dynamics using the unscented kalman filter," in *2018 Annual American Control Conference (ACC)*. IEEE, 2018, pp. 2593–2598.
- [10] S. Jung and T. C. Hsia, "Explicit lateral force control of an autonomous mobile robot with slip," in *2005 IEEE/RSJ International Conference on Intelligent Robots and Systems*. IEEE, 2005, pp. 388–393.
- [11] S. De Pinto, C. Chatzikomis, A. Sorniotti, and G. Mantriota, "Comparison of traction controllers for electric vehicles with on-board drivetrains," *IEEE Transactions on Vehicular Technology*, vol. 66, no. 8, pp. 6715–6727, 2017.
- [12] L. De Novellis, A. Sorniotti, P. Gruber, J. Orus, J.-M. R. Fortun, J. Theunissen, and J. De Smet, "Direct yaw moment control actuated through electric drivetrains and friction brakes: Theoretical design and experimental assessment," *Mechatronics*, vol. 26, pp. 1–15, 2015.
- [13] Y. Wang, L. Yuan, H. Chen, P. Du, and X. Lian, "An anti-slip control strategy with modifying target and torque reallocation for heavy in-wheel motor vehicle," *Proceedings of the Institution of Mechanical Engineers, Part D: Journal of Automobile Engineering*, p. 09544070211063086, 2021.
- [14] J. Zhou, H. Yue, J. Zhang, and H. Wang, "Iterative learning double closed-loop structure for modeling and controller design of output stochastic distribution control systems," *IEEE Transactions on Control Systems Technology*, vol. 22, no. 6, pp. 2261–2276, 2014.
- [15] C. Yin, J.-X. Xu, and Z. Hou, "A high-order internal model based iterative learning control scheme for nonlinear systems with time-varying parameters," *IEEE Transactions on Automatic Control*, vol. 55, no. 11, pp. 2665–2670, 2010.
- [16] K.-H. Park, "An average operator-based pd-type iterative learning control for variable initial state error," *IEEE Transactions on Automatic Control*, vol. 50, no. 6, pp. 865–869, 2005.
- [17] I. D. Landau, R. Lozano, M. M'Saad, and A. Karimi, *Adaptive control: algorithms, analysis and applications*. Springer Science & Business Media, 2011.
- [18] G. Bai, Y. Meng, L. Liu, W. Luo, and Q. Gu, "Review and comparison of path tracking based on model predictive control," *Electronics*, vol. 8, no. 10, p. 1077, 2019.
- [19] F. Borrelli, A. Bemporad, M. Fodor, and D. Hrovat, "An mpc/hybrid system approach to traction control," *IEEE Transactions on Control Systems Technology*, vol. 14, no. 3, pp. 541–552, 2006.
- [20] P. Falcone, F. Borrelli, J. Asgari, H. E. Tseng, and D. Hrovat, "Predictive active steering control for autonomous vehicle systems," *IEEE Transactions on control systems technology*, vol. 15, no. 3, pp. 566–580, 2007.
- [21] O. Barbarisi, G. Palmieri, S. Scala, and L. Glielmo, "Ltv-mpc for yaw rate control and side slip control with dynamically constrained differential braking," *European Journal of Control*, vol. 15, no. 3-4, pp. 468–479, 2009.
- [22] B. Leng, L. Xiong, Z. Yu, K. Sun, and M. Liu, "Robust variable structure anti-slip control method of a distributed drive electric vehicle," *IEEE Access*, vol. 8, pp. 162 196–162 208, 2020.
- [23] T. Brüdigam, M. Olbrich, D. Wollherr, and M. Leibold, "Stochastic model predictive control with a safety guarantee for automated driving," *IEEE Transactions on Intelligent Vehicles*, pp. 1–1, 2021.
- [24] A. Carvalho, Y. Gao, S. Lefevre, and F. Borrelli, "Stochastic predictive control of autonomous vehicles in uncertain environments," in *12th International Symposium on Advanced Vehicle Control*, 2014, pp. 712–719.
- [25] G. Siddharth, Z. Wang, H. Jing, and Y. Nakahira, "Adaptive safe control for driving in uncertain environments," *arXiv preprint*, 2022.
- [26] A. Clark, "Control barrier functions for complete and incomplete information stochastic systems," in *2019 American Control Conference (ACC)*. IEEE, 2019, pp. 2928–2935.
- [27] W. Luo, W. Sun, and A. Kapoor, "Multi-robot collision avoidance under uncertainty with probabilistic safety barrier certificates," *Advances in Neural Information Processing Systems*, vol. 33, pp. 372–383, 2020.
- [28] P. Falcone, H. Eric Tseng, F. Borrelli, J. Asgari, and D. Hrovat, "Mpc-based yaw and lateral stabilisation via active front steering and braking," *Vehicle System Dynamics*, vol. 46, no. S1, pp. 611–628, 2008.
- [29] H. Zhao, B. Ren, H. Chen, and W. Deng, "Model predictive control allocation for stability improvement of four-wheel drive electric vehicles in critical driving condition," *IET Control Theory & Applications*, vol. 9, no. 18, pp. 2688–2696, 2015.
- [30] E. Siampis, E. Velenis, S. Gariuolo, and S. Longo, "A real-time nonlinear model predictive control strategy for stabilization of an electric vehicle at the limits of handling," *IEEE Transactions on Control Systems Technology*, vol. 26, no. 6, pp. 1982–1994, 2017.
- [31] J. Yoon, W. Cho, J. Kang, B. Koo, and K. Yi, "Design and evaluation of a unified chassis control system for rollover prevention and vehicle stability improvement on a virtual test track," *Control Engineering Practice*, vol. 18, no. 6, pp. 585–597, 2010.
- [32] M. Ataei, A. Khajepour, and S. Jeon, "Model predictive control for integrated lateral stability, traction/braking control, and rollover prevention of electric vehicles," *Vehicle system dynamics*, vol. 58, no. 1, pp. 49–73, 2020.
- [33] M. Isaksson Palmqvist, "Model predictive control for autonomous driving of a truck," <https://www.diva-portal.org/smash/get/diva2:930995/FULLTEXT01.pdf>, 2016.
- [34] U. Kiencke and L. Nielsen, "Automotive control systems: for engine, driveline, and vehicle," 2000.
- [35] P. Falcone, M. Tufo, F. Borrelli, J. Asgari, and H. E. Tseng, "A linear time varying model predictive control approach to the integrated vehicle dynamics control problem in autonomous systems," in *2007 46th IEEE Conference on Decision and Control*. IEEE, 2007, pp. 2980–2985.
- [36] J. A. Andersson, J. V. Frasch, M. Vukov, and M. Diehl, "A condensing algorithm for nonlinear mpc with a quadratic runtime in horizon length," *Automatica*, pp. 97–100, 2013.
- [37] L. T. Biegler, "Efficient solution of dynamic optimization and nmpc problems," in *Nonlinear model predictive control*. Springer, 2000, pp. 219–243.